CUMERI

Customised membranes for green and resilient industries

Models for membrane down-selection

Deliverable D3.3

This project has received funding from the European Union's Horizon Europe Research and Innovation programme under Grant Agreement No. 101091812.

CUMERI

DELIVERABLE REPORT

Start date of project :	December 01, 2022
Duration of project :	36 months
Deliverable n° and name :	D3.3: Models for membrane down-selection
Document n°:	
Version :	Final
Work package n° :	WP3
Due date of D :	July 31, 2024
Actual date of D :	September 30, 2024
Participant responsible :	VITO
Main authors :	Mohammed Nazeer, Recep Kaya, Marcus Weyd, Anita Buekenhoudt, Alan Perez

Nature of the Deliverable		
R	Document, report (excluding the periodic and final reports)	X
DEM	Demonstrator, pilot, prototype, plan designs	
DEC	Websites, patents filing, press & media actions, videos, etc	
DATA	Data sets, microdata, etc.	
DMP	Data management plan	
ETHICS	Deliverables related to ethics issues.	
SECURITY	Deliverables related to security issues	
OTHER	Software, technical diagram, algorithms, models etc.	

Dissemination level		
PU	Public, fully open, e.g. web (Deliverables flagged as public will be automatically published in CORDIS project's page)	X
SEN	Sensitive, limited under the conditions of the Grant Agreement	
Classified R-UE	EU RESTRICTED under the Commission Decision No2015/444	
Classified C-UE	EU CONFIDENTIAL under the Commission Decision No2015/444	
Classified S-UE	EU SECRET under the Commission Decision No2015/444	

Quality procedure			
Date	**Version**	**Reviewers**	**Comments**
2024-09-24		Main modelling partners GS and LT Line	Adding/updating text
2024-09-30	Final	Anita Buekenhoudt	Homogenization and final check overall document

TABLE OF CONTENTS

LIST OF PARTNERS

N°	Name	Short name	Country
1	VLAAMSE INSTELLING VOOR TECHNOLOGISCH ONDERZOEK N.V.	VITO	Belgium
2	FRAUNHOFER GESELLSCHAFT ZUR FORDERUNG DER ANGEWANDTEN FORSCHUNG EV	IKTS	Germany
3	FUNDACION TECNALIA RESEARCH & INNOVATION	TEC	Spain
4	UNIVERSITEIT MAASTRICHT	UM	Netherlands
5	ISTANBUL TEKNIK UNIVERSITESI	MEMT	Turkey
6	SINTEF AS	SINTEF	Norway
7	OSILUB	OSIL	France
8	EREGLI DEMIR VE CELIK FABRIKALARI TURK AS	ERDE	Turkey
9	ERDEMIR MUHENDISLIK YONETIM VE DANISMANLIK HIZMETLERI AS	ERMU	Turkey
10	SAINT-GOBAIN CENTRE DE RECHERCHES ET D'ETUDES EUROPEEN	SGOB	France
11	RAUSCHERT KLOSTER VEILSDORF GMBH	RKV	Germany
12	B4PLASTICS	B4P	Belgium
13	A-MEMBRANES	AMEM	Belgium
14	MEMSIS CEVRE TEKNOLOJILERI ARASTIRMA VE GELISTIRME LIMITED SIRKETI	MEMS	Turkey
15	EUROQUALITY SARL	EQY	France
16	FACHHOCHSCHULE NORDWESTSCHWEIZ	FHNW	Switzerland

PROJECT SUMMARY

This report is part of the deliverables from the project "CUMERI" which has received funding from the European Union's Horizon Europe research and innovation program under grant agreement No. 101091812.

Increased energy and resource efficiency in industrial sectors is paramount to build a resilient and sustainable future. In this context, the CUMERI project will develop and demonstrate at TRL7 **advanced and customized membrane separation systems in two key industries**: in the steel sector where H_2 will be recovered and CO_2 captured in one comprehensive system, and in the O&G industry where a twostep liquid filtration system will enable base oil and additives recovery from used lubricant oil. To reach these goals, CUMERI gathers 16 partners (7 RTOs and 9 companies including 4 SMEs) and will elaborate in 36 months three impactful membrane technologies: 1) Enhanced bio-based and recyclable polymer membranes for CO_2 permeation; 2) Stable and selective SiC/SiCN membranes for H_2 recovery, for a better H_2 valorization in the steel sector; 3) Grafted porous ceramic membranes for waste oil purification and additives recovery by ultrafiltration and liquid-liquid membrane contactors. All membrane systems will unlock greater energy efficiency and decreased emissions in their respective sectors. High separation performances together with increased chemical, mechanical and thermal stability will be demonstrated. Moreover, reusage and recycling of membranes will be validated. Beyond these demonstrations, the project will generate novel insights on membrane separation including a variety of flexible solutions to help industry, the scientific community and policy makers accelerate the rollout of separation technologies. To maximize the impact of CUMERI, other promising separations will be screened and the transferability of results to other industries (refinery, pharmaceuticals, etc.) will be ensured. Through its activities, CUMERI will pave the way to decreased emissions in the industry, to the greater valorization of valuable chemicals, and to more energy-efficient processes, promoting resilient and circular industrial value chains.

OBJECTIVE AND EXECUTIVE SUMMARY

CUMERI focusses on the development and demonstration of advanced and customized membrane separation systems in two key industries for separation tasks in liquid and gaseous media. For proper piloting of the liquid and gas separation processes at the end of this 3 year project, down-selection of the membranes required for piloting is needed. This down-selection is not only performed by experimental test work alone, however, it is supported by different types of modelling. This public deliverable describes the different ways in which modelling was used by the consortium to help selecting the best processes, membranes and modules for upscaling in WP4, and pilot demonstration in WP5.

1. TARGET PROCESSES TO BE PILOTED

Making industry more resilient and meeting the challenge of climate neutrality has become a growing concern, at the heart of the European Green Deal objectives. Customized membranes, tailored to the application can help answering to such objectives. The CUMERI project will in particular pave the way for 1) effective recycling and reuse of valuable components, promoting resilient and circular industrial value chains, 2) more energy-efficient processes, while 3) lowering CO_2 emissions. This will be achieved in two different separation lines: **gas separation** (GS) in the steel industry for the recovery of H_2 and for CO_2 capture, and **liquid treatment** (LT) in the oil and gas (O&G) industry for the recovery of base oil and additives from used lubricant oils (ULO). The recovery of H_2 in the steel industry is attractive as it is expensive and extensively used in the steel-making production (reduction reactions). The recovery of ULO and additives is economically attractive in terms of high-value resource conservation and environment protection, also in a post-fossil era.

In the gas separation line, two platform membrane technologies are finetuned for H_2 recovery and CO_2 capture. On the one hand, nano- and microporous **SiC/SiCN membranes** on oxide free ceramic supports and intermediate layers are finetuned for H_2 permeance. On the other hand, 100 % biobased polyether-block-amide, **PEBA polymer membranes** are designed for CO_2 permeance and high CO_2/N_2 selectivity. Synthesis and down-selection of these membranes has been performed in WP2 and WP3.

In the liquid treatment line, for energy-lean recovery of base oil and additives from ULO, a two-step process consisting of ultrafiltration (UF) followed by membrane extraction (ME) is targeted. For both steps, customized membranes are developed and down-selected in WP2 and WP3. Focus is on **tailored ceramic membrane supports** chemically modified with the right **grafting technology**.

Figure 1 schematically summarizes the two target processes of the CUMERI project, and the different membrane platforms that are used to realize the target processes.

Figure 1 - Target Processes to be piloted in the CUMERI project

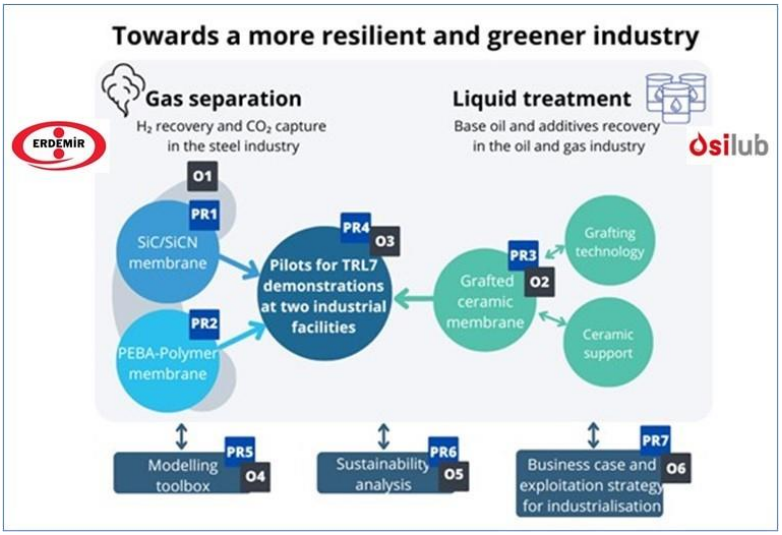

For efficient down-selection of the different membranes, modules and processes, next to extensive experimentation, also **a broad variety of modelling tools** was used. How this modelling supports the final down-selection is described in this public Deliverable D3.3.

2. OVERVIEW OF CUMERI MODELLING TOOLS

A variety of modelling activities in CUMERI have provided guidance for the development of all type of customized membranes and membrane systems with improved performances. The following list gives an overview:

1. Aspen modelling was used in support of the preliminary sustainability assessment (TEA and LCA) and has resulted in first conclusions for the separation systems, described in public deliverable D1.1 Similar modelling will be used for the final assessments.
2. CFD modelling was used to analyse mass transfer through supports and intermediate layers for optimizing ceramic support structures for UF of viscous streams.
3. Simulation was used to define the optimal module configuration for the PEBA membrane gas separation pilot.
4. CFD modelling was used by MEMT to simulate gas flow in the PEBA modules, and suggested the use of a conical shaped element in the inlet of all modules to avoid unnecessary turbulence.
5. DOE (Design of Experiments) was used to perform a more efficient experimental study on UF filtration parameters for ULO treatment
6. HSPs (Hansen solubility parameters) of grafted membranes is calculated and used to quantify membrane affinity, and to correlate with flux and water retention of grafted membranes.
7. UF flux equations allowed VITO to simulate the evolution with temperature (influenced mainly by viscosity) and cross-flow velocity (laminar flow).
8. Film theory was used to understand and simulate the evolution of UF membrane flux with filtration parameters and volume concentration factor. This helps to simulate and predict flux evolution at pilot scale, even for filtration parameters that cannot be reached at lab scale.
9. Rigorous mass-transfer models for ME extraction of metal and additives are being used by FHNW to evaluate ME performance and optimize the process in terms of process parameters, membrane characteristics (pore size and thickness), as well as hydrodynamics. In addition, the model helps in scaling-up the process.

In the following sections each modelling activity is described in more details revealing how it supported down-selection of the different membranes, modules and/or processes.

3. HOW MODELLING SUPPORTS CUMERI

3.1 Aspen modelling assisting TEA and LCA (VITO)

CUMERI targets the development of customized membrane separation systems for liquid and gas treatment applications in two major industries. To evaluate the economic and environmental impacts of the proposed processes, Life Cycle Assessment (LCA) and Techno-economic Assessment (TEA) pre-analysis were conducted in the first 6 months of the project. This initial sustainability analysis relied on defining the value chains, collecting the needed data, and performing mass and energy balance calculations.

This preliminary TEA and LCA assessment for both liquid and gas treatment lines is performed based on **simplified process flow diagrams** (PFD) and **mass and energy balances** defined from the preliminary process design. This is done both for the benchmark processes and for the CUMERI membrane-based alternatives shown in Figures 2 and 3. All information is then directly integrated into a dynamic economic and environmental cost-benefit analysis, giving a first comparison of benchmark and CUMERI processes. Sensitivity analysis further helps to determine the most important parameters influencing cost and environmental impact. The full procedure is described in the earlier CUMERI public deliverable D1.1.

The mass and energy balances for the gas treatment line were mostly obtained through **Aspen plus** simulations. Unlike the OSILUB benchmark facility for liquid treatment line, a proper benchmark for gas treatment line was absent. Therefore, a suitable benchmark was proposed in the CUMERI project which consists of existing commercial processes such as pressure swing adsorption (PSA) and MEA scrubbing process (MEA) for separating hydrogen and capturing carbon dioxide, respectively. The gas treatment line begins with a gas cleaning unit followed by a compressor and a cooler for bringing the cleaned coke oven gas (COG) gas to the required pressure (10 bar) and temperature (30 °C) suitable for PSA where hydrogen is separated. The remaining COG is heated to a higher temperature (100 °C) using a heater block for the oxy-combustion unit (assumed as an equilibrium reactor) which has a constant supply of high-purity oxygen. The flue gas from the oxy-combustion unit at 2500 °C is used in a heat recovery steam generator (HRSG) to produce steam that can be used as an energy source in other processes such as MEA scrubbing. The outlet from the HRSG, still at 200 °C, is cooled to 30 °C to remove the condensed water using a flash separator block. Lastly, the CO_2 is captured in the MEA scrubbing process while a part of the remaining gas is recycled to the oxy-combustion process to restrict the maximum combustion temperature to 2500 °C. The gas cleaning unit, PSA and MEA scrubbing processes were modelled in Aspen Plus as separator blocks. The cost and energy data for these units were obtained from the literature. The rest of the equipment was mapped and sized to estimate the costs using the Aspen process economic analyser. The CUMERI membrane-based process was also similarly modelled in Aspen Plus. The only difference is that the PSA is replaced by a SiC/SiCN membrane module to separate hydrogen and a PEBA membrane module to capture CO_2.

Using Aspen Plus for modelling these value chains allowed a deeper understanding of the energy-intensive steps, sources of emissions, and cost drivers. It also allowed us to fill in and complement the missing data for techno-economic and life-cycle assessments. Similar Aspen plus modelling will be used to assist the final TEA and LCA of the selected gas and liquid treatment processes, later in the project. Specifically for the liquid treatment line, Aspen Plus will be used to model the solvent recovery system and other important equipment such as pre-heaters, coolers, and pumps to obtain accurate estimates of their energy consumption and equipment costs.

Figure 2 – Simplified process flow diagrams for (top) benchmark process, (bottom) membrane alternative for the Liquid Treatment Line

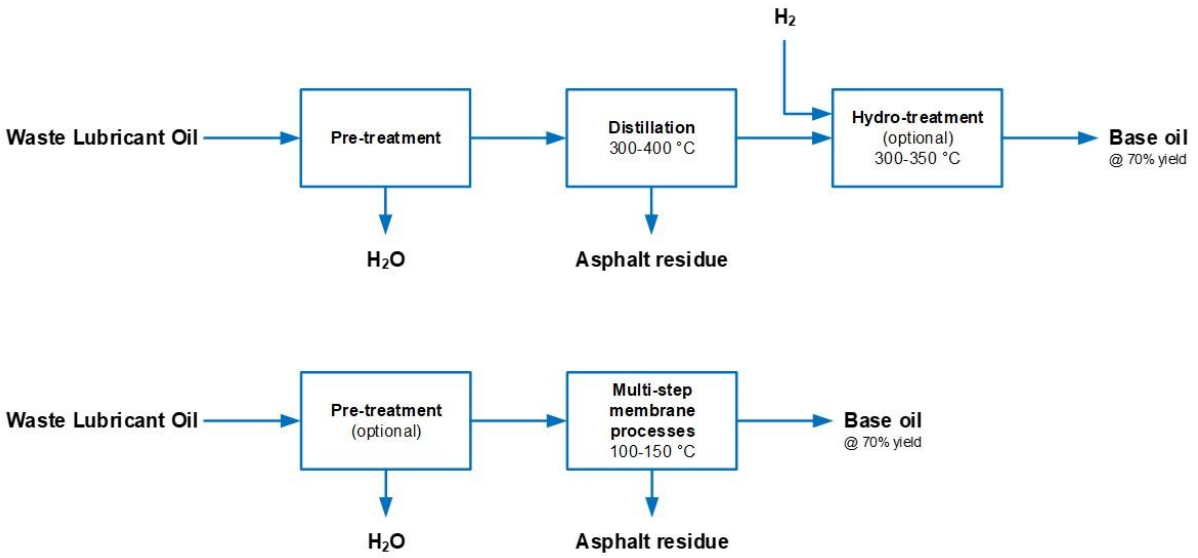

Figure 3 – Simplified process flow diagrams for (bottom) benchmark process, (top) membrane alternative for the Gas Separation Line

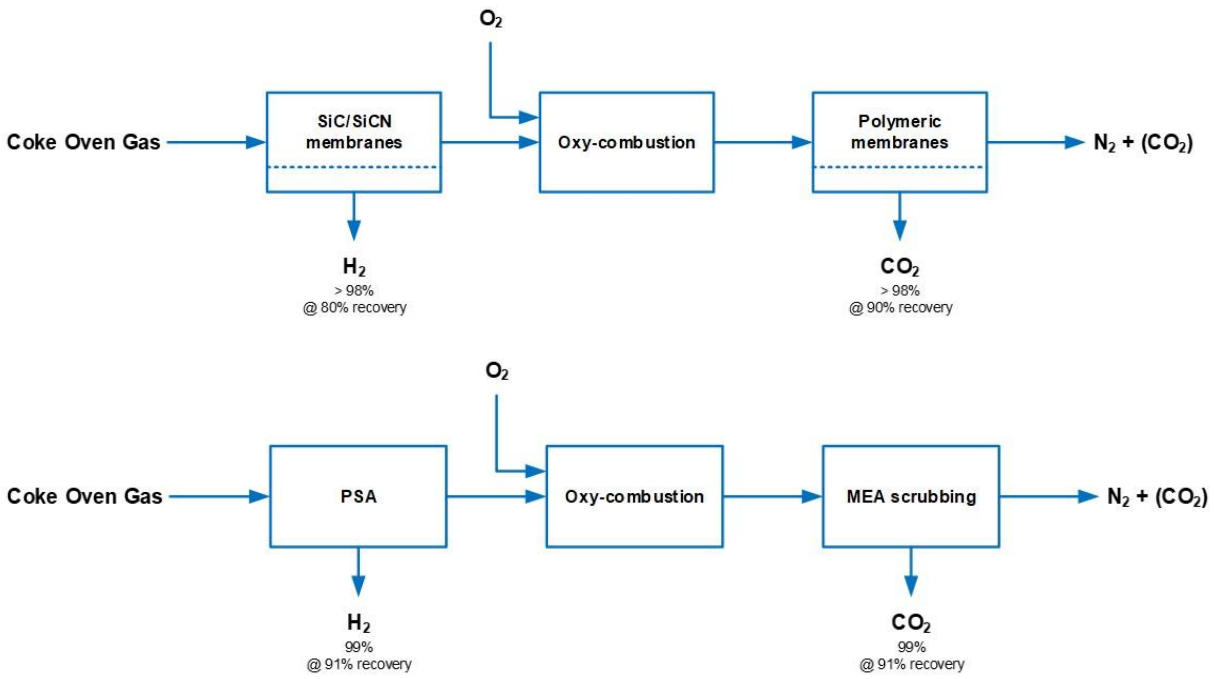

3.2 CFD modelling for UF membrane support evaluation (IKTS)

Ceramic tubular membranes for liquid filtration consist of a porous extruded and sintered porous ceramic tube ("support"), intermediate layers with decreasing pore diameters and a final layer. The final layer can be native one or can be functionalized in order to adapt the surface properties. For lab scale application typically single channel tubular membranes are considered, for industrial application multi-channel membranes, e.g. 19-channel membranes, are considered.

The typical layer characteristics of the used membranes are the following:

- Support: 3 µm pore size, 30 % open porosity, thickness 1.5 mm (for single channel tube)
- 1st intermediate layer: 800 nm pore size, 40 – 45 % open porosity, thickness 20 – 25 µm
- 2nd intermediate layer: 200 nm pore size, 40 – 45 % open porosity, thickness 15 – 20 µm,
- 3rd intermediate layer: 70 nm pore size, 40 – 45 % open porosity, thickness 15 – 20 µm
- Active layer, e.g. 10 nm pore size, 45 % open porosity, thickness around 2 µm

For the typical membrane structure with a final pore diameter of 10 nm water permeation tests were performed with the support and the support subsequently coated with (intermediate) layers. Basing on these data of the support and the following layer structure permeability data were calculated.

Based on the permeability data the flow behaviour (membrane permeance, pressure loss) of more complex membrane structures, e.g. 19 channel membranes can be simulated (Figure 4). Furthermore, flow behaviour for different media can be simulated taking the relevant media viscosity into account.

Figure 4: Simulation room/model and pressure gradient during permeation of water inside out for single channel (left) and nineteen channel membranes.

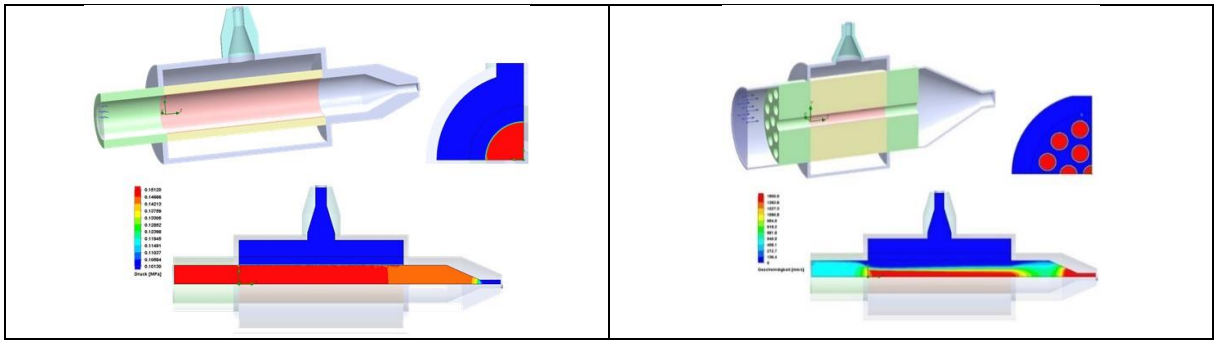

Looking on the pressure gradient over the membrane cross section in single and 19 channel membranes coated with a 10 nm layer the main pressure loss is seen in the thin layer structure for both geometries.

For comparing and simulating flow behaviour of oils, mass transfer simulations were performed using the viscosity of water, of SAE20 oil at 20 °C and of oil at 100 °C. Also for the higher viscous media the main pressure drop can be found in the layer structure (Figure 5). However, the much higher viscosity leads to a clear drop of permeate flux (137 → 1.5 l/(m²hbar) when changing from water to cold oil), especially at low temperature. This is a strong argument for investigating behaviour at higher temperatures/lower viscosity. Further simulation work will be done for adapted viscosity of real oils at relevant temperature and in accordance with the aspired filtration process temperature at pilot scale.

Figure 5: Simulated pressure and flow behavior of a 10 nm single channel membrane during permeation of water and SAE20 oil at two different temperatures.

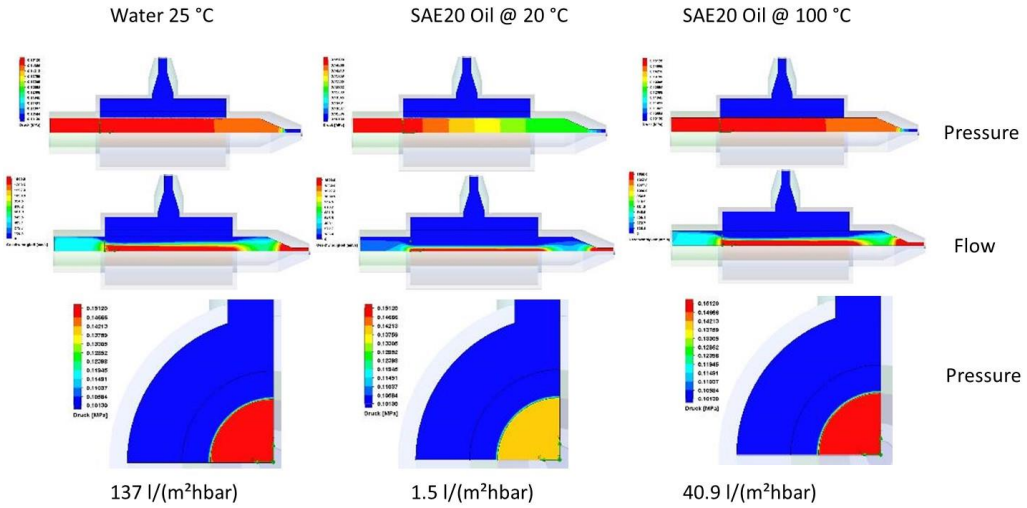

Simulations and evaluation on mass transfer through the layered membrane cross section have shown that the main pressure loss is caused by the finer intermediate and final active layers for single channel and also multi-channel geometries. This allows choosing existing high purity alumina support materials having 3 µm pore sizes and showing high mechanical and chemical stability. These membrane materials allow high temperature applications. The viscosity decrease achieved by high process temperatures is advantageous for membrane permeation and transport of feed through the channels of the membrane hence allowing multi-channel membrane with channel diameters below 5 mm. Practical investigations will show practical usability of multi-channel membranes having different channel sizes, as 3.5 mm for 19 channel tubes and 6 mm for seven channel tubes.

3.3 Simulation to define optimal PEBA-module configuration (MEMT)

The gas separation pilot is expected to integrate about 25 m^2 PEBA polymeric membranes for CO_2 separation. The foreseen capacity is 4 Nm^3/h. Advantageous for the CO_2 separation, the PEBA polymeric membranes will be produced in hollow fibre form, with the toplayer on the inner side. Membrane modules packing a high number of PEBA hollow fibres will be assembled in parallel and the required total membrane area is calculated according with the expected membrane properties.

Modules are planned to be in 4" shells. Each 4" module having approximately 6 m^2 membrane area and total of 4 modules in parallel will be used, to reach the total surface area of near 25 m^2. Based on the estimated hollow fibre dimensions, the membrane area and packing density specs were calculated, and are given in the table 1 below.

Table 1– PEBA membrane module area parameters

4" Module with 1 mm PEBA Hollow Fibers		
Membrane outer diameter (estimated)	**1**	mm
Membrane inner diameter (estimated)	**0.8**	mm
Membrane length	900	mm
Membrane number	2536	number
Membrane surface area	5736296	mm^2
Membrane surface area	**5,74**	m^2
Packing density		
Total membrane cross sectional area	1992	
Whole 4" tube circle cross sectional area	7854	
Packing density	**25**	(%)

Based on these simulations, detailed design of the PEBA membrane pilot module plant piping and instrumentation was completed. The 3D design of both modules and P&ID can be found in Figure 6.

Figure 6: PEBA membrane pilot module plant piping and instrumentation

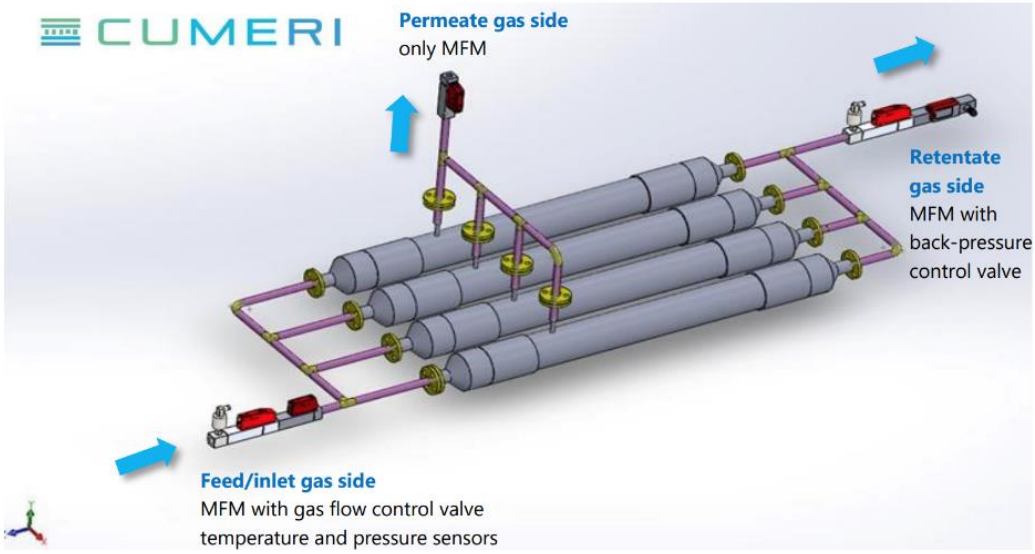

3.4 CFD modelling to simulate gas flow in PEBA modules (MEMT)

The PEBA modules considered for the gas separation pilot of CUMERI have been modeled and flow simulation has been done using CFD modelling. According to the gas flow inside the module, a few design modifications have been made and checked by using CFD simulation. The possible design modifications have also been applied to the CFD simulation. General boundary conditions for the CFD modelling have been given in table 2 below.

Table 2– Boundary conditions for the PEBA modules used in CFD modelling

Domain	Boundaries	
Gas	Boundary - inlet	
	Type	Velocity inlet
	Location	Inlet 4 Nm3/h at 10 Bar
	Boundary - outlet	
	Type	Pressure outlet
	Location	Outlet - 0 Pa

Velocity streamlines at the inlet port of the 4" modules, as calculated by CFD modelling, can be seen in figure 7.

Figure 7: CFD flow simulation of a PEBA membrane pilot module

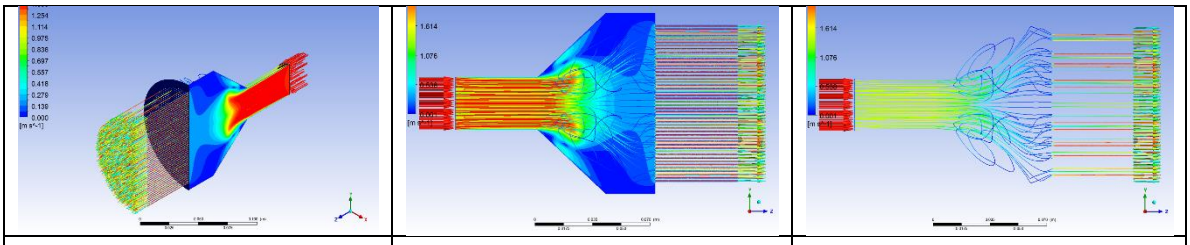

Velocity distribution at inlet	Velocity distribution & streamlines	Velocity streamlines
4 Nm3/h – 1.393 m/s @ 10 Bar		

The velocity streamlines for the designed hollow fiber membrane modules have shown that turbulent flow at the inlet side of the 4" module creates unnecessary turbulence. The gas flow entering to the small hollow fiber openings (1- or 2-mm diameter) creates especially uneven flow at the inlet cap.

To overcome this unnecessary turbulence at the inlet, a diamond shaped cone was placed inside the inlet port space. CFD simulations belonging to this modification can be found in the Figure 8 and 9.

Figure 8: CFD flow simulation of a PEBA membrane pilot module with cone modification1

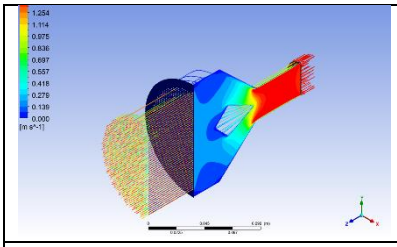	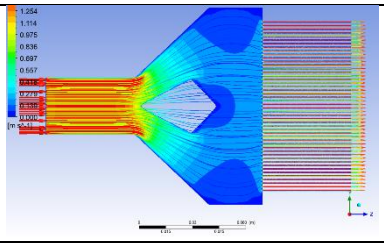	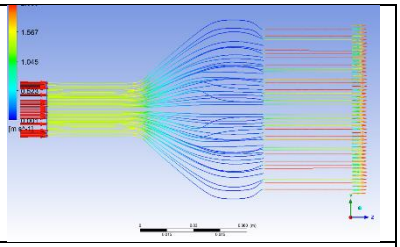
Velocity distribution at inlet	Velocity distribution & streamlines	Velocity streamlines
4 Nm3/h – 1.393 m/s @ 10 Bar with cone-1 modification		

Figure 9: CFD flow simulation of a PEBA membrane pilot module with cone modification2

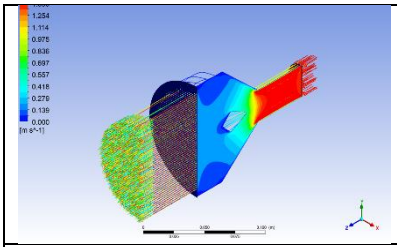	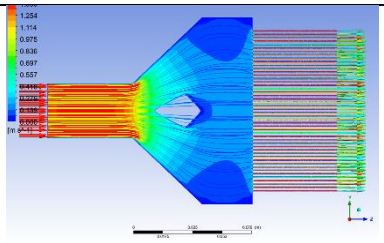	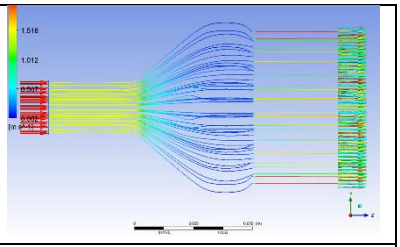
Velocity distribution at inlet	Velocity distribution & streamlines	Velocity streamlines
4 Nm3/h – 1.393 m/s @ 10 Bar with cone-2 modification		

Without modifications, the space at the inlet creates unnecessary turbulence, and this turbulence entanglement can increase during longer periods of membrane run time because of the membrane clogging.

Conical shapes placed inside the inlet space can regulate the unnecessary turbulence at the inlet and create an even more equal distribution of the gas flow coming into the hollow fibers.

The CFD modelling results allowed to define the preferred cone modification to be used during the pilot module assembly.

3.5 DOE to define optimized UF filtration parameters (VITO)

UF flux values for a specific membrane at a specific temperature are dependent on transmembrane pressure (TMP) and cross-flow velocity (CFV) used during the filtration. This is also the case for the UF fluxes of (grafted) ceramic membranes when used for used lubricant oil filtration (ULO) at temperatures near 100°C in CUMERI. To study the influence of both parameters efficiently and derive their optimal values, design of experiments (DOE) was used.

DOE is a systematic method that enables scientists and engineers to study the relationship between multiple input variables (i.e. factors, in casu TMP and CFV) and key output variables (i.e. responses, in casu Flux). By manipulating multiple inputs at the same time, DOE can identify important interactions that may be missed when experimenting with one factor at a time, and leads more efficiently to the most optimal combination of factors to maximize the response. DOE leads to a set of experiments defined by the high and low levels of the different input variable. In this case:

- TMP low and high levels are 9 and 16 bar
- CFV low and high levels are 1.8 and 3.2 m/s

These values have been inspired by previous experimentation, and technical limitations in lab- and pilot-scale equipment.

Different statistical methods can be used in DOE to design the efficient set of experiments. In CUMERI VITO has used Response Surface Methodology using MiniTab®, leading to the UF test set of Table 3. Repetitions are automatically build in, as well as some variables slightly outside the low/high levels.

Table 3– Set of UF experiments defined by DOE

RunOrder	Type	CFV	TMP
1	axial	1.8	12.5
2	axial	3.2	12.5
3	axial	2.5	9
4	axial	2.5	16
5	center	2.5	12.5
6	corner	2	15
7	center	2.5	12.5
8	corner	2	10
9	center	2.5	12.5
10	corner	3	15
11	corner	3	10
12	center	2.5	12.5
13	center	2.5	12.5

This same set of experiments has been used to test a down-selected series of ceramic (grafted) UF membranes. Figure 10 shows an example of the results in 3D. Figure 11 shows cross-sections at CFV 2,5 m/s, and at different TMPs. The results of all membranes are very similar and revealed that a limiting flux at TMP above about 10 bar, and a limiting flux value that increases with CFV. The DOE has allowed to define, for every membrane, the optimal TMP (where the limiting flux plateau starts) for each CFV. Higher TMPs are not recommendable as they only increase fouling, without increasing flux. This limiting flux behavior is typical for concentration polarization or cake layer formation, and can be modelled by the thin-film theory, as is also the case for the CUMERI UF filtration data (shown in section 3.8).

Figure 10: Typical UF flux evolution with TMP and CFV. Y-axis does not start at 0.

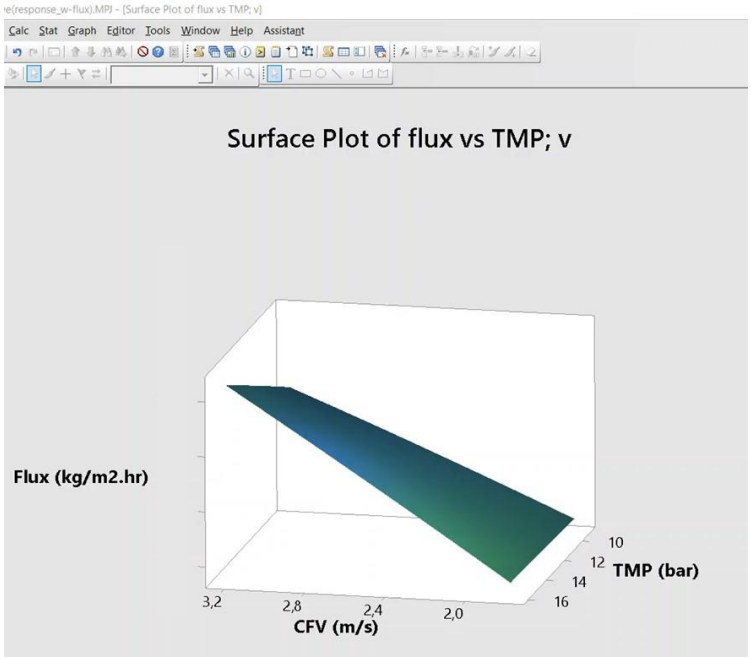

Figure 11: UF flux as function of TMP for CFV = 2.5 m/s for one particular membrane (top), and UF flux as function of CFV for different TMPs for another membrane (bottom). Y-axes are the same in both graphs.

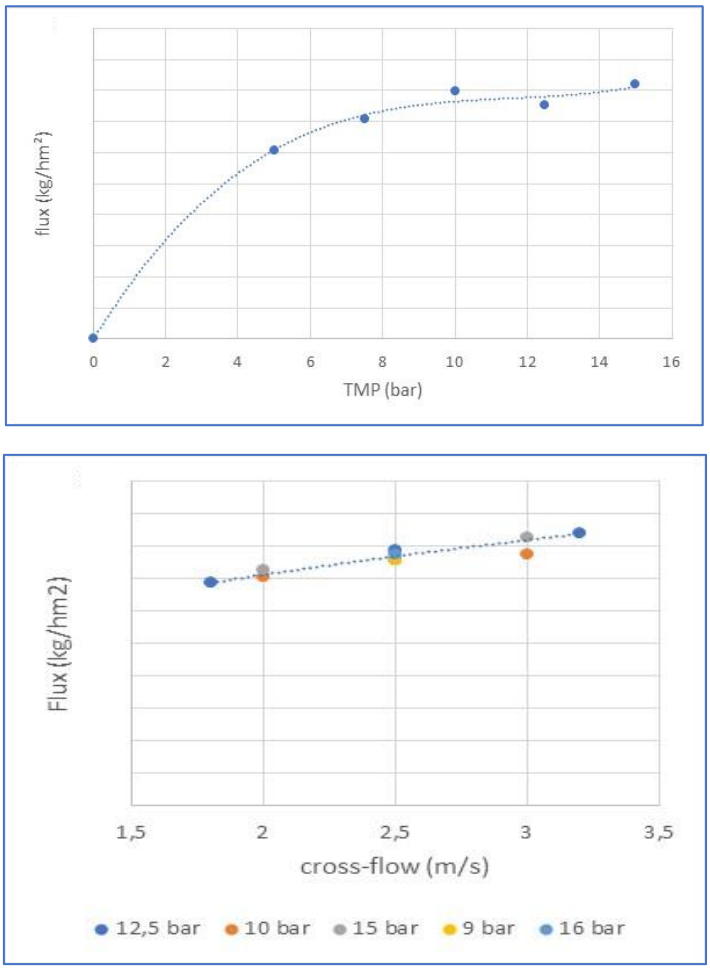

3.6 Hansen Solubility Parameters to quantify UF membrane affinity (VITO)

Hansen Solubility Parameters (HSPs) quantify the potential of molecules to interact with each other, and thus also with others. Interactions are possible via different forces, as dispersion or van de Waals (d), polar (p) or hydrogen-bonding (h) interactions. As a consequence, the total HSP (tot) of a molecule consists of 3 contributions determined by the 3 type of interactions [HSP]:

$HSP_{tot}^2 = HSP_d^2 + HSP_p^2 + HSP_h^2$

As a consequence, HSPs can be represented as a point in a 3D space. HSPs have proven to be a powerful, practical way to understand issues of solubility, dispersion, diffusion, chromatography and more. For instance a solute that has HSP values very similar to those of a solvent (points in the 3D space close to each other) is very well soluble in this solvent. HSP values can not only be defined for solutes and solvents, but also for solids (based on their solubility or affinity in a range of different solvents).

VITO has shown that HSPs are also powerful tools to understand complex membrane performance. For instance, HSPs of solvents and solutes help to understand organic solvent nanofiltration with ceramic membranes [Andecochea Saiz, 2018]. Other have shown that HSPs can help to select good pervaporation membranes for a specific application [Buckley-Smith, 2006].

In CUMERI we have produced and tested ceramic UF membranes with a wide variety of surface chemistries, in order to find the optimal membrane for UF filtration of Used Lubricant Oil (ULO). The variety in surface chemistries was created by grafting membranes in many different ways. Partner IKTS used silanation. VITO used Grignard grafting or grafting of small polymer chains Surface Initiated Atom Transfer Radical Polymerization (SI-ATRP). UF test results of these many membranes have shown a strong variation in UF oil flux and in retention of the water in the used oil (one of the impurities in ULO). Further, the permeate quality, for instance the retention of the metal impurities (coming from lubricant additives and from wear) and of acidity and oxidation products in the ULO, is almost the same.

The HSP values of the (grafted) membranes were calculated in order to quantify their affinity to oil and water in the following way:

- For native membranes, the HSP values (close to water) derived in [Andecochea Saiz, 2018] were used
- For Grignard grafted membranes, the method described in [Andecochea Saiz, 2018] taking into account partial coverage of the surface by grafted groups and remaining OH groups, was used
- For SI-ATRP grafted membranes, HSP values of the grafted polymer was calculated using the HSPiP software [HSPiP].
- For the membranes silanated using long perfluoroalkyl silanes, the HSP values of PTFE calculated by the HSPiP software, were used.

Figure 12 plots the polar and hydrogen bonding HSP values for all membrane chemistry types prepared within CUMERI. The color code determines the values of the dispersion HSP (blue: 14-16, orange 16-18, green 18-20, black 20-22 $MPa^{1/2}$).

Figure 12 shows that the membranes synthesized and tested in CUMERI span a wide variety of surface chemistries, ranging from the very hydrophilic native membranes with high HSP_p and HSP_h (right top corner of the plot), to very hydrophobic grafted membranes with low HSP_p and HSP_h (low bottom corner of the plot). For comparison we have also marked the water HSP values (open diamond) and the mineral oil HSP values (open square) [HSP mineral oil], positioned each on one side of the plot.

The membrane HSP values were used to look for correlations with the flux and water retention of each membrane. This revealed that not only membrane chemistry plays a role, but also membrane pore size. This study allowed to select membranes that combine high flux and high water removal rates. It pointed also to further directed investigations required to better understand the UF performance variations.

Figure 12: Plot of HSP values for all UF membranes synthesized within CUMERI. HSP_d is defined by different colors (see text, in rising order: blue, orange, green, black). HSP values of mineral oil and water are added for comparison.

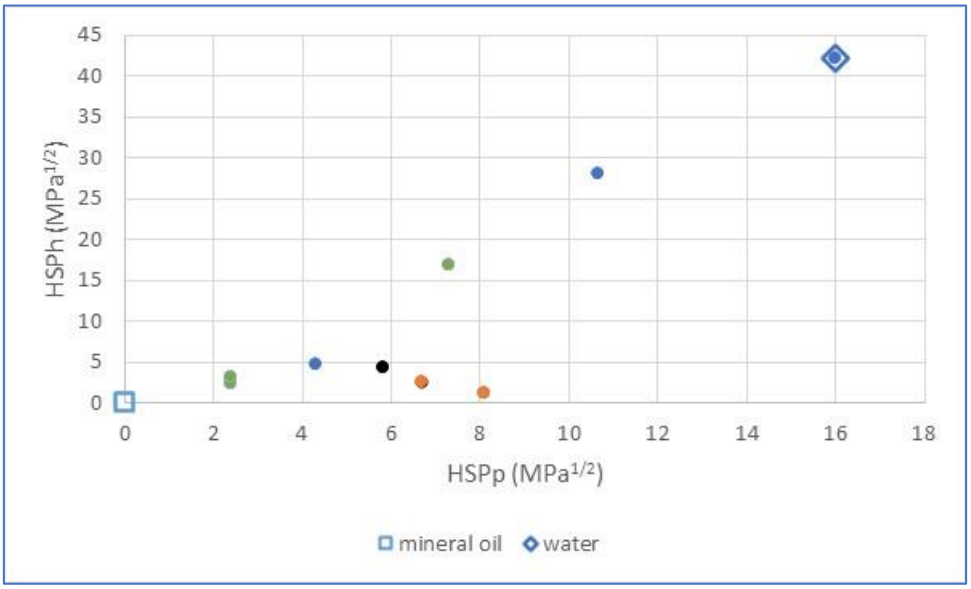

References:

[Andecochea Saiz, 2018]: J. Membr. Sci. 546 (2018) 120

[Buckley-Smith, 2006]: PhD thesis, University of Waikato, 2006

[HSP]: http://hansen-solubility.com/

[HSP mineral oil]: http://hansen-solubility.com/HSP-examples/cleaning.php/

[HSPiP]: http://hansen-solubility.com/HSPiP/

3.7 UF modelling simulating temperature and cross-flow evolution (VITO)

UF process flux cannot only be optimized by selection of the right membrane, but also by using the optimal process conditions of temperature, transmembrane pressure (TMP) and cross-flow (CFV).

The effect of temperature has been studied at the CUMERI standard ULO filtration conditions, being TMP of 10 bar, and CFV of 2 m/s. Temperature was varied between 80 and 120°C. Figure 13 shows the results, and emphasizes the strong influence of temperature on the UF flux: flux increases with more than a factor 2 when the temperature rises from 80 to 120°C. According to the Hagen-Poiseuille equation, temperature dependence in UF filtration is inversely proportional to the dynamic viscosity of the transporting liquid, this is the permeate.

It is important to notice that in this particular case of ULO filtration, there is quite some difference between the viscosity of the feed (kinematic viscosity typically 55 cSt at 40°) and the viscosity of the permeate (kinematic viscosity typically 24 cSt at 40°C). Thanks to the extensive analysis of all filtration samples, also the viscosity index and density was determined of all permeates, and we can calculate the dynamic viscosity at each temperature. As can be observed from Figure 13, the evolution the UF flux with temperature perfectly matches the evolution of 1/viscosity for the permeate.

This allows us to simulate the flux that can be obtained at higher temperatures (not obtainable in the VITO lab-scale set-ups), as the 130°C that is reachable with the VITO UF pilot that will be used in CUMERI, or even 150°C in case an adapted equipment would be used/build. These values are also input for the detailed economic and environmental analysis that is performed in the project.

Figure 13: Typical UF flux evolution with temperature (points) and simulation using the temperature dependence of the dynamic viscosity.

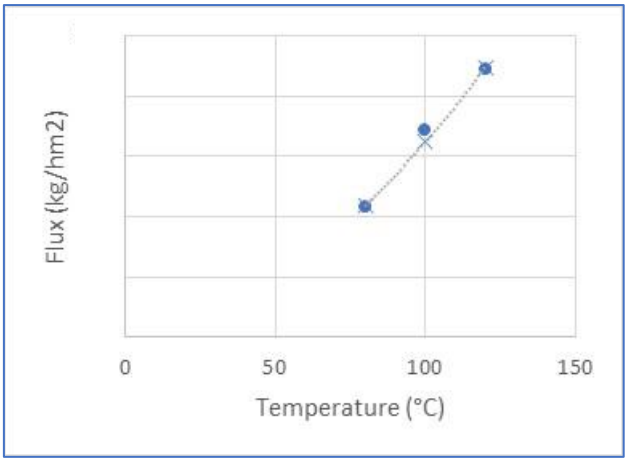

In section 3.5, the effect of cross-flow velocity on UF flux was already shown. Figure 13 shows 2 extra graphs elucidating that the influence of cross-flow follows a power law with an exponential close to 1/3, and this independent of the membrane used, or TMP or temperature used. This particular $CFV^{1/3}$ variation fits to laminar flow conditions (Reynold numbers < 2000), typically met for high viscous liquids as ULO [Noble, 1995]. This allows us again to simulate ULO fluxes in other conditions than those tested at lab-scale. It emphasizes also the importance of high cross-flow conditions to reach high enough fluxes. We calculated that for the VITO UF pilot, CFV of 2 m/s will be reachable even at high ULO concentration factors.

Figure 14: Typical UF flux evolution with cross-flow (points) and simulation revealing laminar flow behavior (dotted line).

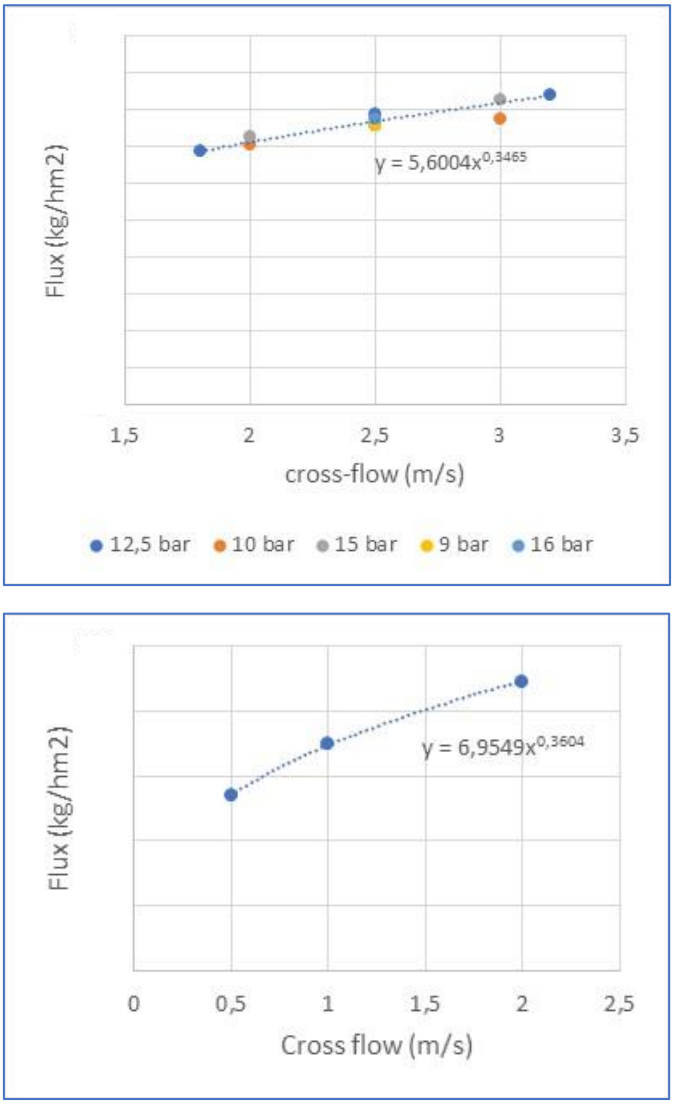

Reference:

[Noble]: Book, Membrane Separation Technologies, Principles and Applications, Noble and Stern, Elsevier 1995

3.8 UF modelling simulating flux decline during concentration (VITO)

The film theory describes the evolution of the flux during an UF filtration, when a concentration layer of the retained solutes is building up. According to this theory the UF flux J is described by the following equation [Wijmans, 1984]:

$J = k \ln [(cm - cp) / (cb - cp)]$

with k the mass transfer coefficient of the membrane at the specific filtration conditions used, cm the concentration of impurities at the membrane surface, cp their concentration in the permeate, and cb their concentration in the bulk of the retentate/feed. For filtration at specific conditions, cm will increase fast at the start of the filtration, until a so called "gel-layer" is formed. From that moment onwards the flux is constant and defined by the concentration in the formed gel-layer cg:

$J_{lim} = k \ln [(cg - cp) / (cb - cp)]$

This flux is also often called the limiting flux J_{lim}.

This is exactly what we see in the UF filtration of ceramic membranes in ULO: as soon as the temperature reaches the intended high value (> 100°C) and the transmembrane pressure TMP is imposed, a stable flux is reached almost instantaneously (see Figure 15). This flux is typically much lower than the flux of clean base oil with the same membrane at the same conditions.

Figure 15: Typical UF flux measurement showing instantaneous stable flux

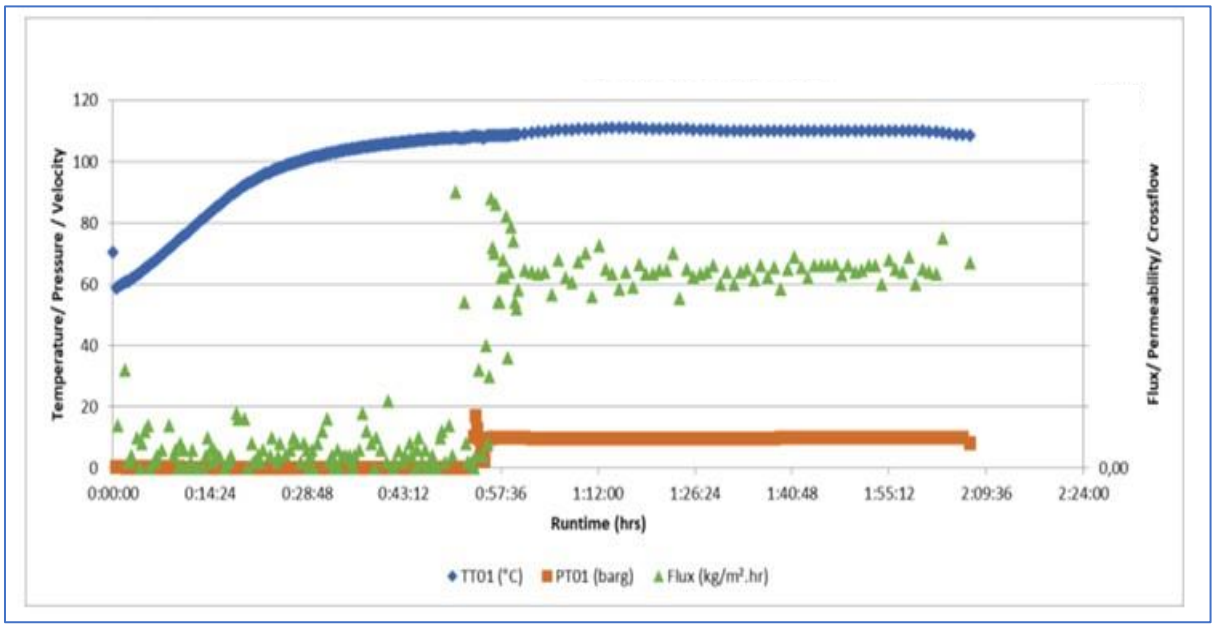

During an ULO concentration track the UF flux is decreasing due to the further increase of the bulk concentration of the impurities retained at the feed/retentate side, cb. The following figure 16 shows this behavior. Remark that the flux decline is rather limited considering the volume concentration factor VCF reached (near 3).

To keep the cross-flow velocity during this test constant at the optimal 2 m/s, this test was done on a single tubular membrane (for multichannel membranes VITO's lab-scale installation cannot keep the 2 m/s at high concentration factors). Remark that the pumps of the pilot installation at VITO are big enough to keep the 2 m/s even for 8 large multichannel membranes as intended to be used during pilot demonstration in CUMERI.

Figure 16: Typical UF flux evolution during concentration up to factor 3.

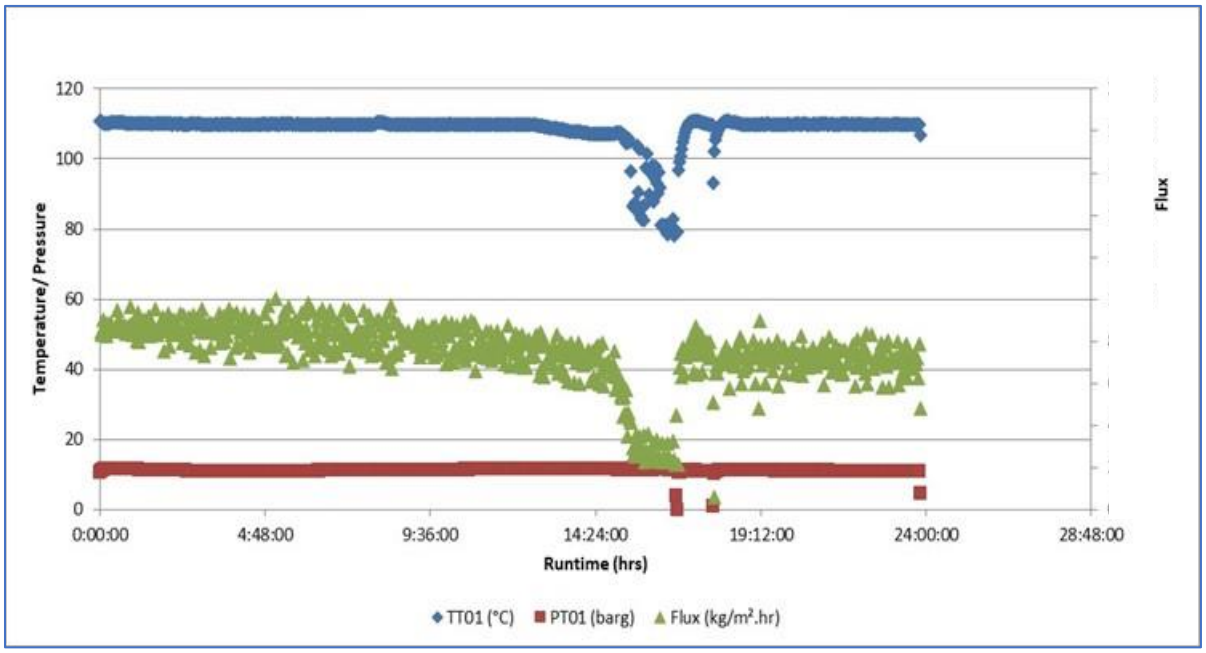

During the concentration tests also different samples were taken, and their analysis has shown the following results that allow us to simplify the theoretical expected J_{lim} evolution with increasing cb:

- Permeate quality is constant during concentration, meaning that cp is constant
- Also viscosity of the permeate stays constant during concentration, meaning that the mass transfer coefficient k for the used membrane is constant during the concentration
- Moreover, UF membranes retain impurities in the ULO quite well so that cp << cg and cb

This allows to reduce the J_{lim} equation to:

$$J_{lim} = k \ln (cg/cb)$$

Moreover, we know that during concentration with a fixed retention R, cb = cf VCF^R with cf the concentration of impurities in the ULO feed. As a consequence we can derive the expected evolution of the UF flux with VCF during concentration, if the film theory applies :

$$J_{lim} = k \ln (cg/cf) - k R \ln (VCF)$$

The first factor is a constant, leading to a flux evolution that is linearly changing with ln (VCF). This is exactly what we can derive from flux curves like the one in Figure 16, and is shown in Figure 17 and proved by the high R2 number of the linear fit.

We have shown that this same linear evolution with ln (VCF) applies to all different types of membranes tested. This includes membranes with different pore sizes, as well as different chemistries (obtained by grafting). The fitting parameters do evolve logically with pore size and membrane chemistry. The fitting parameters for a specific membrane as measured for a small-scale membrane, can be used to predict the behavior at the pilot demonstration with a number of large-scale versions of this membrane.

Figure 17: Typical UF flux evolution during concentration up to VCF 3

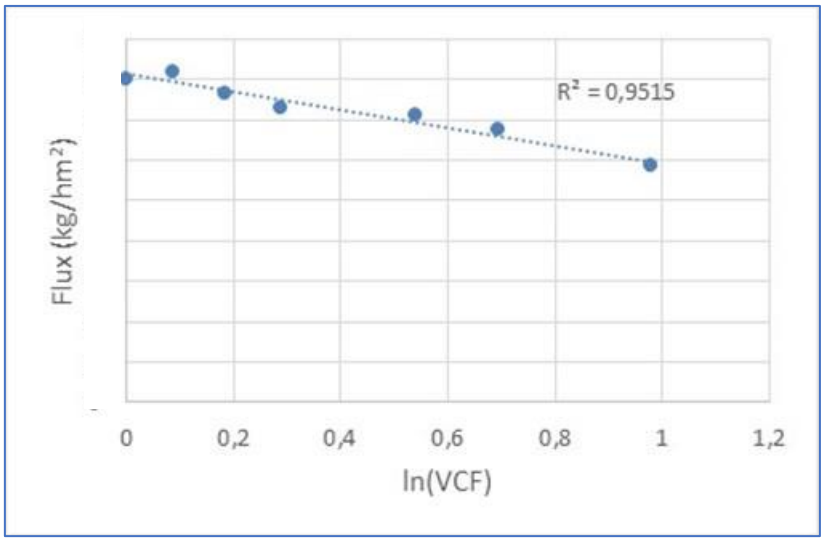

Reference

[Wijmans, 1984]: J. Membr. Sci., 20 (1984) 115

3.9 Modelling of ME mass transport (FHNW)

The derivation of the mathematical model describing the mass transport of one or more compounds from the feed (liquid containing the target compounds to be removed) to the solvent phase (liquid that can selectively extract the target compounds from the feed) is based on the general mass balance (equation 1) over the control volume of the system (within the membrane contactor) for each component involved. The derived equation depends on the type of operation (co-current or counter-current, batch or continuous) and the location of the fluids (feed and solvent) in the membrane extraction module (shell or lumen).

$$\begin{pmatrix} Mass\ flow\ rate \\ of\ component\ i \\ into\ the\ system \end{pmatrix} - \begin{pmatrix} Mass\ flow\ rate \\ of\ component\ i \\ out\ the\ system \end{pmatrix} + \begin{pmatrix} Mass\ rate\ of\ generation \\ of\ component\ i \\ due\ to\ chemical\ reaction \end{pmatrix} = \begin{pmatrix} Mass\ rate\ of\ accumulation \\ of\ component\ i \\ in\ the\ system \end{pmatrix} \quad \text{Eq. 1}$$

The derivation of the mathematical model will be developed for several cases. For all cases considered here, no chemical reaction is assumed. Therefore, the generation term in the mass balances is zero for all cases shown below.

3.9.1 Mass transport model in a loop-wise membrane extraction configuration (quantification of K_{ov}-value)

In loop-wise operation, both feed and solvent flow in a closed loop. Therefore, from an experimental point of view, the decrease in concentration of the target compounds in the feed phase can be followed over time (by sampling and measuring the concentration of target compounds), while the increase in concentration of the target compounds in the solvent phase can be followed either by calculation (using mass balances) or by analytical quantification (by sampling this phase and measuring the concentration of target compounds of each sample) over time until saturation is reached (or close to it).

The benefit of the loop-wise approach is that several operating conditions or different membranes or different membrane operations can be tested to evaluate the performance of the membrane extraction under specific conditions by calculating the overall mass transfer coefficient (K_{ov}) after each experiment.

To calculate the K_{ov} value, it is necessary to combine the experimental data and the mathematical model, which describes the change in concentration of target compounds over time in a membrane extraction process, in a loop-wise operation. The mathematical model for membrane extraction in loop-wise operation is derived as follows.

Consider a tube-in-tube membrane extraction module as shown in Figure 18 (left is the operation sketch, while in right side is the flow within the membrane extraction module). The inner tube is a hollow fiber or capillary porous membrane, and the outer tube is the housing (or shell) of the membrane extraction module. Let's consider also that the feed phase flows inside the inner tube (lumen side) while the solvent flows in the space between the inner and outer tubes (shell side). This means that the mass transport of target compounds is from the lumen side (where the feed phase is located) to the shell side (where the solvent phase is located).

Figure 18: Loop membrane extraction (left) and internal view of a tube-in-tube membrane extraction module operating in a closed loop (right).

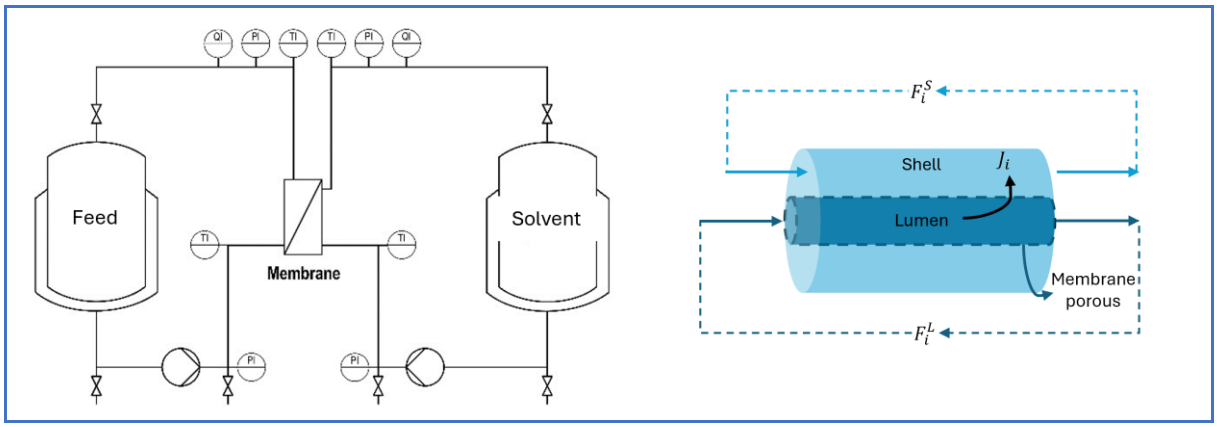

From the previous considerations, the mass balances (in shell side and in lumen side) are like a batch operation as there is no inlet or outlet flow when the feed and solvent phases flow in a closed loop. In addition, the flux transport of the solute i from feed to solvent phase (J_i term in Figure 18) is described by thin film theory as shown in Equation 2 [Ref1].

$$J_i = K_{ov,i} \cdot \Delta C_i \qquad \text{Eq. 2}$$

For the specific case where the feed phase (used lubricant oil) flows in the lumen side and the solvent (ethanol) flows in the shell side, equation 2 can be rewritten as follows:

$$J_i = K_{ov,i} \cdot \left(C_{i,feed} - \frac{C_{i,solvent}}{D} \right) \qquad \text{Eq. 3}$$

$$D = \frac{C^*_{i,solvent}}{C^*_{i,feed}} \qquad \text{Eq. 4}$$

Where $K_{ov,i}$ is the overall mass transfer coefficient for the component i (that is transported from feed to solvent), $C_{i,feed}$ is the concentration of component i in the bulk of feed phase, $C_{i,solvent}$ is the concentration of component i in the bulk of solvent phase, and D is the distribution coefficient of substance i between feed and solvent (described in equation 4).

Assuming a negligible change in volume of the feed in lumen side (V_L) and solvent in shell side (V_S) phases during the extraction process, the mass balances in the shell and lumen are described as follows:

$$-V_L \frac{dC_i^L}{dt} = J_i \cdot A_m \qquad \text{Eq. 5}$$

$$C_i^L(t=0) = C_{i,0}^L \qquad \text{Eq. 6}$$

$$V_S \frac{dC_i^S}{dt} = J_i \cdot A_m \qquad \text{Eq. 7}$$

$$C_i^S(t=0) = C_{i,0}^S \qquad \text{Eq. 8}$$

Where C_i^L is the concentration of component i at time t in feed phase (lumen side) and $C_{i,0}^L$ is the initial concentration of component i (at t = 0) in feed phase. Similarly, C_i^S is the concentration of component i at time t in solvent phase (shell side), $C_{i,0}^S$ is the initial concentration of component i (at t = 0) in solvent phase. A_m is the contact area provided by the membrane and can be calculated as follows:

$$A_m = 2 \cdot \pi \cdot R \cdot L \cdot N_t \quad \text{Eq. 9}$$

Where L and R are the length and the radius of the membrane tube, respectively. The inner radius must be considered when the wetting phase which is in the shell side (in this case, the solvent) fills the pores of the membrane, and the outer radius must be considered when the wetting phase is in the lumen side (in this case, feed).

The term N_t, indicates the number of tubes, for the case of a tube-in-a tube approach membrane extraction module, where N_t is one (N_t = 1), but in the case of a multi-tubular approach (as shown in Figure 19), the number of tubes must be considered for the calculation of the membrane area as showed in equation 9.

Figure 19: Internal view of a multi-tubular membrane extraction module operating in a closed loop.

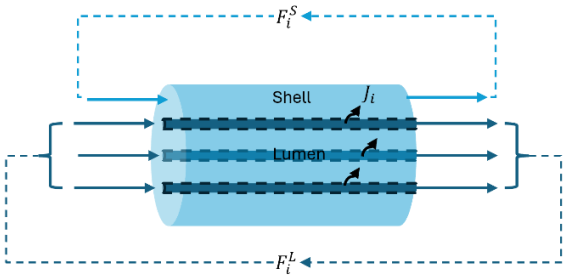

The system of algebraic ordinary differential equations consisting of the set of equations 3-9 must be solved simultaneously as an initial value problem (IVP).

The K_{ov} value provides information on the performance of a specific membrane extraction system and its operating conditions. Therefore, a loop-wise approach membrane extraction setup is a useful tool to evaluate the performance of a membrane without having a significant large membrane area, as the experiment can be run to saturation and by following the concentration of the target compounds in the feed and/or solvent phase and combining it with the model given by equations 3-9, the K_{ov} value can be calculated.

At the FHNW, K_{ov} values of about $1*10^{-7}$ to $1*10^{-8}$ m/s have been found for different membrane extraction processes, such as lactic acid membrane extraction and caprolactam membrane extraction [Refs 2 and 3]. Therefore, it is presumed that the K_{ov} value for the membrane extraction of used lubricating oil to ethanol might be in this range.

Figure 20 shows the predicted (by the above shown model) sulfur concentration in the oil phase during a membrane extraction process with ethanol at two expected K_{ov} values (continuous lines in Figure 20), while comparing them with experimental results (squares in Figure 20) carried out at FHNW under proper hydrodynamic conditions, operating the system at 50 °C, using a hydrophobized ceramic membrane with pore size 200 nm, and a membrane area of 0.011 m^2 (OD = 10 mm and ID = 7 mm, with a porosity of 40-45%) under 14 days (which is also proving to be a stable process).

Figure 20: Typical predictions of the concentration profile for sulfur in the worst case (continuous blue line) and best case (continuous red line) and some typical experimental data (yellow squares) during membrane extraction with ethanol at 50 °C.

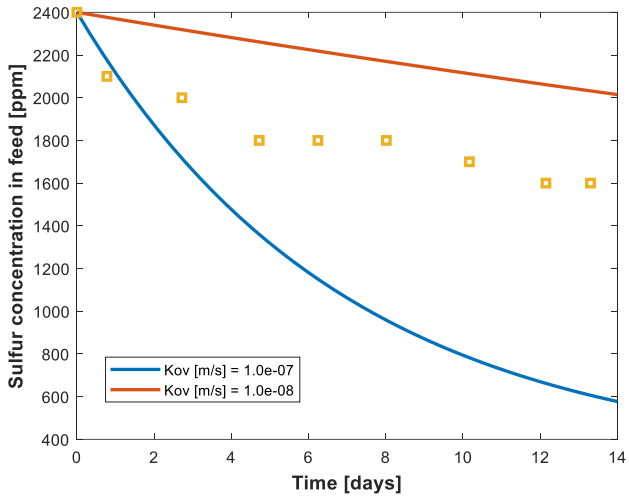

On the one hand, the modelling results showed that the assumption that the Kov value for sulfur removal is in the range of $1*10^{-7}$ to $1*10^{-8}$ m/s under certain conditions is correct, since the obtained experimental results are within this range. It also clear, that there still chance of improvement on the K_{ov} value higher value of K_{ov} value), by optimizing the operating conditions of the membrane extraction system, by combination of experiments and the model derived in this section.

References:

[Ref 1] Riedl,W., Mollet, D., Grundler, G.: Using Membrane-Supportes Liquid-Liquid Extraction for the Measurement of Extraction Kinetics, Chimia 2011, 65 (5)

[Ref 2] A. Gössi, W. Riedl and B. Schuur, Chemical Engineering Science: X 13 (2022) 100119

[Ref 3] Riedl, W. (2002). Membrangestützte Flüssig-Flüssig-Extraktion bei de Caprolactamherstellung. Universität Erlangen-Nürnberg.

3.9.2 ME continuous counter-current model and predictions/estimations

The development of a continuous and countercurrent model for membrane extraction of additives from ULO to ethanol is important as this mode of operation is commonly used on an industrial scale.

To derive the mathematical model for a continuous and countercurrent membrane extraction process, the control volume of Figure 21 in a differential length of the membrane module was considered for the mass balance (one in lumen side, and another in the shell side) of the involved compounds.

Figure 21: Internal view of a differential tube segment in a tube membrane extraction module operating in countercurrent and continuous modes.

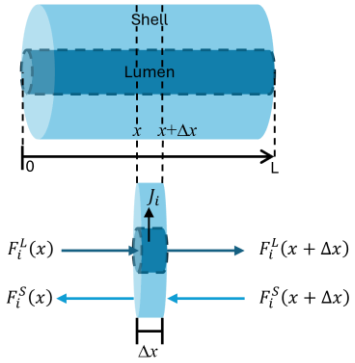

The set of equations 10-14 in combination with equation 3, comprises a system of algebraic ordinary differential equations that describes the change in concentration of the additives in used lubricant oil (located in lumen side) during the membrane extraction process using a proper solvent (flowing in the shell side). The above-mentioned set of equations must be solved as a boundary value problem (BVP), since an initial condition (equation 12) and a final condition (equation 14) are known. The differential equations 11 and 13 can be solved from left ($x = 0$) to right ($x = L$) or from right to left. In both cases an initial condition is missing. Therefore, an iterative numerical method is useful in this case to solve the BVP.

$$P_m = 2 \cdot \pi \cdot R \cdot N_t \quad \text{Eq. 10}$$

$$-Q^L \frac{dC_i^L}{dx} = J_i \cdot P_m \quad \text{Eq. 11}$$

$$C_i^L(x = 0) = C_{i,0}^L \quad \text{Eq. 12}$$

$$-Q^S \frac{dC_i^S}{dx} = J_i \cdot P_m \quad \text{Eq. 13}$$

$$C_i^S(x = L) = C_{i,L}^S \quad \text{Eq. 14}$$

In the previous set of equations, P_m is the perimeter of the membrane tube given by equation 15, and R inner radius of the membrane when the wetting phase is on the shell side or R is the outer radius of the membrane when the wetting phase is on the lumen side. The total volumetric flow Q^L in lumen side (in this case ULO) and total volumetric flow Q^S in the shell side are considered for the model operating in continuous.

The K_{ov} value is a key parameter that must be known to solve the BVP above. Therefore, once the K_{ov} value is calculated from the loop-wise approach, it can be inserted into the continuous and countercurrent modeling to predict the change in concentration of the target compounds and determine the required length (or area) for a specific target removal.

3.9.3 ME semi-batch model and predictions/estimations

Another operational alternative that can be scaled up for membrane extraction of additives from ULO is semi-batch operation, an approach that operates continuously but in batches. This is possible when the target removal in continuous is split over a day. For example, it is necessary to process 250 L/day of ULO where the sulfur concentration in the ULO needs to be reduced from 3000 ppm to 300 ppm (90% removal) as shown in Figure 22. Here, 250 L (V_L in equation 5) of ULO can be processed in batch over 24 hours. If every 24 hours are processed 250 L of ULO, the sum of all batches works as continuous.

Therefore, the model developed for wise loop (batch) given by the equations 3-9 can be implemented here.

To solve the IVP given by the previous set of equations, we now include the constraint of time (24 hours) and the final concentration of sulfur (300 ppm, as an example) as shown in Figure 22. Under the above constraint and knowing the K_{ov} value (the optimum), the IVP is solved iteratively to calculate the membrane area that fully fills all the requirements (the above constraints) of the operation.

Figure 22: Reduction of the sulfur concentration in ULO by membrane extraction from 3000 ppm to 300 ppm in a semi-batch operation (processing 250 L of ULO in 24 hours).

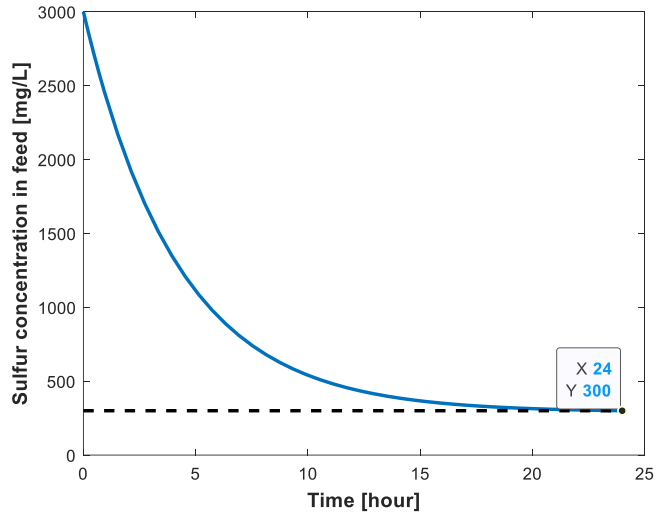

Once the membrane area for a specific target has been calculated in semi-batch mode, it can be compared with the membrane area required for the same target in continuous countercurrent mode. The advantages and disadvantages of each mode can then be quantified in terms of cost.

4. CONCLUSIONS

Several modelling and simulation techniques proved useful to understand mass transfer and/or flow patterns in CUMERI membranes and modules, offering support in down-selections of membranes and processes. Hereby a short summary of the conclusions of the 9 types of modelling used:

1. Aspen Plus modelling was/is used in support of (preliminary) sustainability assessment (TEA and LCA). For both liquid and gas treatment lines calculations are performed based on (simplified) process flow diagrams and mass and energy balances defined from (preliminary) process design of benchmark and alternative membrane-based processes. Using Aspen Plus for modelling these value chains allows deeper understanding of energy-intensive steps, sources of emissions, and cost drivers. It has already resulted in first conclusions for the separation systems, to be refined soon.
2. CFD modelling was used to analyze mass transfer through supports and intermediate layers for optimizing ceramic support structures for UF of viscous streams. Simulations on mass transfer through the layered membrane cross section showed that the main pressure loss is caused by the finer intermediate and final active layers, both for single-channel and multi-channel geometries. This allows choosing existing high purity alumina supports with high mechanical and chemical stability.
3. Simulation was used to define the optimal module configuration for the PEBA membrane gas separation pilot, starting from the geometry of the PEBA hollow fibres and the aimed treatment flows. Calculations show that four 4" modules wil provide the required 25 m^2 of membranes.
4. CFD modelling was used to simulate gas flow in the PEBA modules. This showed that unnecessary turbulence is created at the inlet of standard 4" modules. Similar simulations suggested the use of a conical shaped element in the inlet of all modules to avoid this unwanted turbulence. The modelling also allowed to derive the optimal size of this conical element.
5. DOE (Design of Experiments) was used to perform a more efficient experimental study determining the influence of transmembrane pressure and cross-flow velocity (input parameters) on the UF flux (response) in ULO filtration, and allowed to derive limiting flux behaviour. It results also in optimal values for the input process parameters.
6. HSPiP software was used to calculate the three HSPs (Hansen solubility parameters) of grafted membranes. The resulting values were used to quantify membrane affinity, and to correlate with flux and water retention. They showed the wide variety of membrane chemistries created within CUMERI.
7. Temperature evolution of UF flux follows the variation of the permeate viscosity, as suggested by the Hagen-Poiseuille equation. Flux evolution with cross-flow velocity is predicted by laminar flow equations, characteristic for high viscosity streams. This allows to simulate the flux at temperatures and cross-flows, not obtainable in lab-scale set-ups, but reachable with the VITO UF pilot.
8. Film theory allows to understand the evolution of UF membrane flux during concentration up to high concentration factors (VCF). Thanks to the good and constant permeate quality during concentration, flux decline is limited and evolves with ln (VCF). This helps to simulate and predict flux evolution at pilot scale, even for filtration parameters that cannot be reached at lab scale.
9. Rigorous mass-transfer models for ME extraction of metal and additives from ULO have been developed as follows:
    - Loop-wise model: allows to calculate and optimize ME performance (K_{ov} value).
    - Continuous and countercurrent flow model: provides information to scale up the membrane extraction process (calculate the required membrane area for a specific target removal).
    - Semi-batch model: provides information to scale up the membrane extraction process (calculate the required membrane area for specific target removal) and provide an alternative operation of continuous countercurrent.